The Effect of El Niño on Flood Damages in the Western United States

THOMAS W. CORRINGHAM AND DANIEL R. CAYAN

Scripps Institution of Oceanography, University of California San Diego, La Jolla, California

(Manuscript received 3 July 2018, in final form 25 February 2019)

ABSTRACT

This paper quantifies insured flood losses across the western United States from 1978 to 2017, presenting a spatiotemporal analysis of National Flood Insurance Program (NFIP) daily claims and losses over this period. While considerably lower (only 3.3%) than broader measures of direct damages measured by a National Weather Service (NWS) dataset, NFIP insured losses are highly correlated to the annual damages in the NWS dataset, and the NFIP data provide flood impacts at a fine degree of spatial resolution. The NFIP data reveal that 1% of extreme events, covering wide spatial areas, caused over 66% of total insured losses. Connections between extreme events and El Niño–Southern Oscillation (ENSO) that have been documented in past research are borne out in the insurance data. In coastal Southern California and across the Southwest, El Niño conditions have had a strong effect in producing more frequent and higher magnitudes of insured losses, while La Niña conditions significantly reduce both the frequency and magnitude of losses. In the Pacific Northwest, the opposite pattern appears, although the effect is weaker and less spatially coherent. The persistent evolution of ENSO offers the possibility for property owners, policy makers, and emergency planners and responders that unusually high or low flood damages could be predicted in advance of the primary winter storm period along the West Coast. Within the 40-yr NFIP history, it is found that the multivariate ENSO index would have provided an 8-month look-ahead for heightened damages in Southern California.

1. Introduction

Flooding is the most common and damaging natural disaster in the United States (NOAA/NCEI 2018). Billions of dollars have been spent to reduce the impact of the flood hazard in communities across the country (U.S. Army Corps of Engineers 2009). In spite of these efforts, the average annual economic costs of flooding in the United States have continued to rise. Since the year 2000, direct flood damages averaged $8.6 billion (all amounts in U.S. dollars), excluding storm surge flooding due to hurricanes and tropical storms (NOAA/National Weather Service 2018); dollar figures are inflation-adjusted to 2017 dollars throughout (U.S. Bureau of Economic Analysis 2018). Several factors are responsible for the increasing trend in flood damages, including population growth, income growth, and increased migration toward coastal areas (Villarini and Slater 2017; Glantz 2001; Changnon et al. 2000). There is evidence that global climate change is partly responsible, through increased frequency of hurricanes and tropical storms (Wang et al. 2018; Risser and Wehner 2017; Groisman et al. 2005; Karl and Knight 1998) and an intensification of the hydrologic cycle (Westra et al. 2013; Santer et al. 2007). It is unclear whether federal policies have aggravated the flood problem, or whether the increases in damages have occurred in spite of the success of these programs (Horn and Brown 2018; Kunreuther 1998; Sylves and Waugh 1996). Coming to substantive conclusions is difficult due to the lack of consistent data on flood damages and exposure (Changnon 2003), although the increase in damages in the United States appears to be driven largely by increased exposure (i.e., increased population and wealth in areas at risk of flooding) (Klotzbach et al. 2018; Downton et al. 2005; Pielke et al. 2002; Changnon et al. 2000).

ⓐ Denotes content that is immediately available upon publication as open access.

Corresponding author: Tom Corringham, tcorringham@ucsd.edu

Publisher's Note: This article was revised on 28 June 2019 to correct a mistake in the authors' affiliation and to include an additional acknowledgment in the Acknowledgments section.

An established body of climate research demonstrates the effects of large-scale atmospheric–oceanic oscillations on hydrologic conditions in the western United States (e.g., Dettinger et al. 1998; Cayan et al. 1998; Gershunov and Barnett 1998). El Niño–Southern Oscillation (ENSO) is a recurring interannual global pattern of ocean-climate variability, driven by sea surface temperature and air pressure differentials in the tropical Pacific (Philander 1990). The boreal winter signature phases of the oscillation, El Niño and La Niña, are associated with floods, droughts, and weather disturbances globally.

As they affect North America, El Niño episodes are associated with a deepened, southward-extended Pacific low pressure system, a persistent extended Pacific jet stream, and an amplified storm track that produces unusual wetness across the southern tier of the United States. In contrast, La Niña episodes typically feature anomalous high pressure over the North Pacific, a variable Pacific jet stream, and cool and wet weather in the Pacific Northwest and south of the Great Lakes. Unusually dry and warm weather across the southern tier of the U.S. precipitation in the southwestern United States is significantly enhanced in the El Niño phase, and diminished in the La Niña phase of the oscillation (D'Odorico et al. 2001; Gershunov and Barnett 1998; Redmond and Koch 1991). Beyond seasonal precipitation and mean streamflow conditions, it has been established that large-scale climate variations, including ENSO, influence extreme hydrologic and precipitation events (Emerton et al. 2017; McCabe-Glynn et al. 2016; Ward et al. 2016; Ward et al. 2014a,b; Andrews et al. 2004; Dettinger et al. 2001; Higgins et al. 2000; Cayan et al. 1999; Gershunov 1998; Dettinger et al. 1998; Livezey et al. 1997; Cayan and Peterson 1989; Ropelewski and Halpert 1986).

Advances in climate science have led to an improved understanding of the role of interannual climate variability in virtually all sectors of the economy. For example, ENSO, which is the dominant mode of interseasonal to interannual climate variability, is known to influence agriculture, fisheries, human health, and coastal and terrestrial infrastructure (e.g., Glantz 2001). In the western United States, El Niño has a well-documented effect in directing and intensifying North Pacific winter storms (e.g., Cayan et al. 1999). The strong El Niño events of 1982/83 and 1997/98 have been linked to significantly damaging flooding in Southern California, caused by enhanced precipitation and by increased ocean surface wave activity along the Pacific coast combined with high astronomical tides and an El Niño effect that inflates the water column. Damages have been estimated at over $1.4 billion for each of these two events (Changnon 2003).

However, understanding the connection between extreme hydrologic events and the social and economic impacts of related floods has not received as much attention. The lack of economic data on flood damages has limited research on the economic impacts of climate and hydrologic variability (Changnon 2003). Direct measures of trends in flood-plain occupancy levels or in local flood mitigation investments have not been collected or are not publicly available, and previous analyses linking hydrologic factors to economic damages have been limited to annually aggregated loss series, over large spatial areas, relying on the general assumption that trends in population growth and the increase in real wealth have been spatially homogeneous [e.g., Pielke and Downton (2000) and Sylves (1998); although see, e.g., Czajkowski et al. (2017) for a more sophisticated approach]. Pielke and Downton (2000) investigated annual NWS reported flood damages at the state and regional level, finding significant links between reported flood damages and a variety of hydrologic measures, including, most strongly, the number of two-day top-percentile statewide streamflow events per year. They concluded that more spatially detailed studies would be useful to quantify the spatially varying effects of climate phenomena such as ENSO. There is also growing concern that natural variability and human-caused climate change may cause changes in the timing and intensity of the regional hydrologic cycle resulting in anomalously extreme hydrologic events. Hence, to inform policy-making, a better quantitative understanding is needed of the connections between such hydrologic extremes and the expected economic costs.

In this paper, we investigate ENSO effects on flood damage over the western conterminous United States (Arizona, California, Colorado, Idaho, Montana, Nevada, New Mexico, Oregon, Utah, Washington, and Wyoming). The key dataset, described herein, is a novel source of flood damages: 40 years (January 1978–December 2017) of daily claims and insured losses over the western United States from the National Flood Insurance Program (NFIP). The NFIP data, along with associated climate and hydrologic records, reveal a strong regional and temporal structure in the economic impacts of flooding associated with ENSO-related interannual climate variability.

2. Methodology

Pielke and Downton (2000) distinguish between hydrologic floods, in which observed streamflow or river stage exceeds some threshold value or percentile, and economically damaging floods that cause injury, loss of life, or damage to real property. Clearly all floods are

hydrologic, but not all floods cause extensive damage to property or loss of life. For a given hydrologic flood, damages or impacts are jointly determined by the magnitude of the hydrologic event and by the level of exposure or vulnerability of real assets located in the affected area.

In the present study, the determination of flooding (and flood damage) is made using reports from affected residents, specifically subscribers to the NFIP. Although the analyses are tied to claims and payouts of flood damage, there is an underlying conceptual framework that follows a phenomenological chain. This framework links economic impacts (NFIP claims and insured losses) to location-specific, generally slowly time-varying exposure or vulnerability (population density, real wealth, NFIP participation rates, and coverage levels), to extreme streamflow and surface runoff, to seasonal and spatial patterns of extreme precipitation that are modulated by location-specific topography and physiography, and to temporally and spatially varying climate variability. In the following sections we describe these linkages, with attention to the driving climatic patterns, and with ultimate focus on economic impacts.

3. Data

a. Insured losses and total damages

We obtained NFIP data on flood insurance claims and insured losses (i.e., indemnity payments) for the 11 western states of the conterminous United States. The data cover 40 years, from January 1978 through December 2017, and contain records of 82 588 claims filed, and over $1.6 billion in payments. The NFIP, established by the U.S. Congress in 1968 (42 U.S.C. 4028), is a federal program enabling property owners to purchase insurance protection against losses from flooding. This insurance provides an alternative to ex post disaster assistance to meet the escalating costs of repairing damage to buildings and their contents caused by floods (e.g., Kunreuther 1998) and is part of a broader program designed to reduce exposure to flood risk over the long term.

The NFIP record provides a resource to explore the economic impacts of ENSO across the western United States. The fine spatial and temporal resolution of the data allows us to quantify the economic effects of floods as they relate to a variety of climatic and hydrologic phenomena. As records of total flood impacts, or even of total direct flood damages, the NFIP data are incomplete. Federal flood insurance is available only for residential properties and some small business properties, damages to which constitute only a small fraction of total direct damages (Dixon et al. 2006). In addition, even in Special Flood Hazard Areas (areas in which the estimated annual flood risk is at least 1%, or one event in 100 years) participation in the program is far from universal.

Low participation rates in the early years of the program led to a series of reforms designed to encourage residents in high risk areas to purchase insurance (Horn and Brown 2018; Pasterick 1998). Take-up rates are estimated at less than 50% in the most flood-prone areas, and under 1% elsewhere (Dixon et al. 2006). Damages caused by floods not covered by the NFIP include damage to infrastructure, such as dams, levees, bridges, roads, highways, and rail lines, damage to public and industrial property, and damage to agricultural property, crops, and livestock. Importantly, NFIP losses do not include secondary or indirect costs of floods, such as reduced productivity, unemployment, or flood-related health costs. Also, not included in NFIP losses are losses above policy coverage limits, which were generally $250,000 or less over the sample period.

Despite the above shortcomings, a principal advantage of the NFIP data over other available data sources (e.g., Downton et al. 2005; Sylves 1998) is that they provide a consistent daily record of claims and losses at relatively high spatial resolution. Each claim in the NFIP database is located to the nearest FEMA community, typically an incorporated area (i.e., a census-defined place: city, town, village, county, county remainder, or Native American tribal area). The street address of each claimant is not available, but the NFIP does provide the location of a large number of claims to the nearest census block group (roughly 40 000 claims, or one-half of the claims in our dataset, have block group codes that match the community coding).

For each claim, the NFIP data provide the date of loss (the date on which the most significant damage occurred), the location of the property (FEMA community, and census block group, if available), the occupancy type (single family residential, 2–4 family residential, 5+ family residential, or nonresidential), the flood zone in which the property is located, and the total payment for structural damages and damages to contents. In a supplementary dataset, the (available upon request from the NFIP) annual number of policies in force, coverage levels, and premium payments are available at the community level.

As of policy-year 2017, there were approximately 392 000 policyholders in the 1807 participating NFIP communities in the western 11 states. In 1978 there were less than 144 000 policyholders, whereas at a peak in 1999 there were over 498 000 policyholders. The total coverage in force, in 2017, was just over $118 billion (in year 2017 U.S. dollars). Total premiums paid in 2017

were approximately $292 million, or 0.247% of total coverage in force. This may seem like a low number. However, expected flood losses are generally far lower than total coverage levels; in most areas severe floods are relatively infrequent, and when such floods do occur most losses are not catastrophic. From 1978 to 2017, insured losses per water year (October–September) over the 11 western states ranged from a low of $1.6 million in 1987 to a high of $126 million in 1995. Median insured losses per water year were roughly $19.9 million, while average annual insured losses were $41.7 million. The average policyholder paid $239 for $92,000 in coverage in 1978, and $745 for $301,000 in coverage in 2017 (or $2.60 to $2.47 per $1,000 of coverage respectively).

There is a notable lack of homogeneity in the number of policies, both spatially by community, and temporally, by water year. One possible explanation for the increase in participation through 1999 and subsequent decrease is the "Cover America" marketing campaign of the mid-1990s. There have also been a number of significant reforms of the NFIP over the sample period (1994, 2004, 2012). The increases and decreases in coverage levels vary substantially over time from state to state and even from county to county (results not shown). There are a number of possible explanations. A significant flood event in a community may lead to increased participation, or alternatively residents may drop their insurance after a flood thinking a 100-yr flood is unlikely to happen again in a short time period. Market forces may have significant effects: people may drop their policies during recessions. Federal oversight may be important. Residents in flood plains who hold federally backed mortgages are required to purchase flood insurance, but it is not clear whether this is commonly enforced.

As a rough control for changes in exposure over time and for spatial disparities in coverage levels, we present results both for total insured losses, and for insured losses per $100,000 of coverage in the affected NFIP community. References to loss per coverage indicate this loss metric. Both sets of results are important: total insured loss numbers capture the impacts of flooding on the NFIP; insured losses per coverage provide a correction for the lack of homogeneity in the data and are likely more indicative of patterns and trends in the total damages for which NFIP losses are a proxy.

In several of our analyses we aggregate NFIP data to monthly 0.5° gridded data. The spatial aggregation for insured losses is relatively precise. Roughly half of our data are located to the nearest census block group, and the other half to the nearest county. We aggregate spatially using block group and county centroids rounded to the nearest half degree. Policies, premium payments, and total coverage in force data are only available annually at the NFIP community level, so are aggregated annually to the nearest half degree, again rounding the community centroid to the nearest half degree. Claims and policy data are then merged together for our analyses.

b. Climate data

As a measure of ENSO climate variability, we use the Wolter and Timlin (1998) multivariate ENSO index (MEI), which is a measure constructed using sea surface temperatures, atmospheric pressure, and wind patterns over the Pacific Ocean. We found MEI to be better correlated with insured losses than either the Southern Oscillation index or Niño-3.4 (results not shown). Of the 40 winters in our sample [or extended cool seasons, which we define as the months of October through March (ONDJFM)], average MEI was 0.035. We conduct split-sample analyses of flood insurance claims and insured losses by region against MEI by breaking ONDJFM monthly MEI into upper, lower, and middle terciles, with break points of -0.11 and 0.66. We note that the sample period of 1978 to 2017 is somewhat biased toward El Niño winters over La Niña winters, so the samples used in our split-sample analyses bear a strong but not precise correspondence to traditional measures of El Niño, neutral, and La Niña winters.

4. Results

a. Insured losses versus total flood damages

Given low participation rates in the NFIP in the western United States, an obvious question is how insured losses compare to total flood damages. To answer this question, we compare the NFIP insured losses, aggregated by state and by water year, to annual reports of statewide total damages collected from National Weather Service (NWS) publications (Downton et al. 2005; Pielke and Downton 2000; Sylves 1998). The NWS dataset covers the years of 1983 to 2003 and was derived from NWS Hydrologic Information Center estimates provided under contract to the U.S. Army Corps of Engineers. The data are based on information from newspapers, estimates from emergency managers, insurance agents, and local officials, and, in the case of presidential disaster declarations, from damage assessments by FEMA storm survey teams. Crop damage estimates were obtained from monthly reports on claims made by farmers to the U.S. Department of Agriculture. Losses from the NFIP dataset will be referred to throughout as "insured losses," while
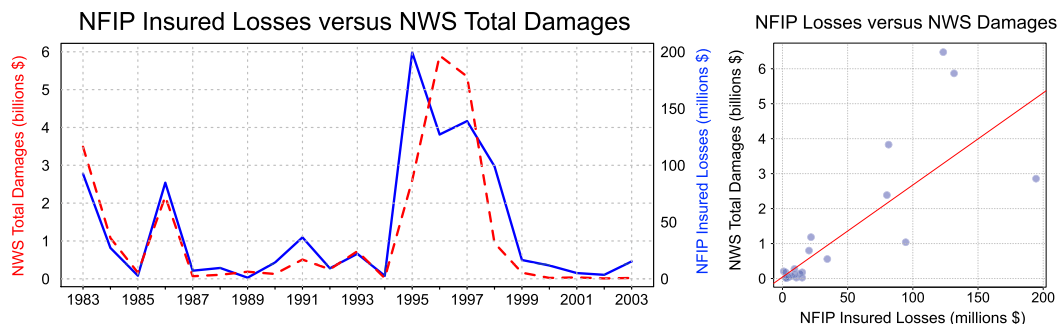
FIG. 1. NFIP insured losses; NWS total damages 1983–2003 western 11 states. (left) Annual aggregates of inflation-adjusted NWS damage estimates (dashed red line) and NFIP insured losses (solid blue line) reveal strong coherence (correlation = 0.8). (right) A scatterplot between NFIP insured losses and NWS total damages shows some variability around the line of best fit.

reported damages from the NWS dataset will be referred to as "total damages."

A comparison of the magnitudes of these two series from 1983 to 2003 (the years for which both NFIP and NWS data were available), as depicted in Fig. 1, reveals that NFIP insured losses summed over the entire western United States were well correlated with the NWS yearly total damages, with the Pearson correlation coefficient registering 0.80 between the two series. As an average over 1983–2003, the magnitude of the NFIP insured losses summed over the 11 western states was 3.3% of total NWS-reported total damages. Following these results, the NFIP insured losses can be inflated by a factor of 30 to obtain a rough estimate of the total damages. For example, the most significant flood events in our sample (e.g., 30 December 2005 and 7 January 1995) caused over $7 million in insured losses: this is equivalent to total damages of $2.25 billion. These estimates of total damages may seem high but are within the expected order of magnitude of such events (i.e., over $1 billion; Perry 2005; Changnon 2003). The high year-to-year variability of the area total damages over the 11 states is symptomatic of the extremely episodic nature of the flood damages exhibited at the daily and local to regional levels, described in more detail below.

In the comparison of 1983–2003 annual NFIP insured losses to annual NWS total damages over the 11 western states, some discrepancies are observed in the years with significant damages (e.g., 1995 and 1996). The high value of NFIP insured losses relative to NWS total damages in 1995 appear to be due to a single event, 9 January 1995, with losses concentrated in Sonoma County, primarily occurring in the residential communities along the lower Russian River. The high value of NWS total damages relative to NFIP insured losses in 1996 appears to be due to extreme damages reported by the NWS in Oregon associated with the Willamette Valley flood,

which caused high nonresidential damages. These discrepancies highlight the need for the collection and consistent archiving of more comprehensive flood impact data.

b. Spatial distribution of insured losses

Insured flood losses by county are presented in Table 1, which lists the counties with the greatest total insured losses over our sample period, in dollar terms, and relative to number of policies and total coverage. The spatial pattern of losses across the entire western United States can be seen graphically in the accompanying Fig. 2. A strong link between population and losses is apparent, but population is not the sole source of exposure to flood risk. In terms of insured losses, many counties in California ranked highly, with mean annual losses exceeding $1 million. In terms of insured losses per coverage, the pattern is less spatially coherent. In particular, insured losses in Southern California, which were high in absolute terms, were relatively low in terms of total coverage, or the number of policies. This is likely due to the high population density of Southern California and high NFIP penetration levels.

There were some areas that showed high insured losses both in dollar values and in insured losses per coverage. These included counties surrounding Puget Sound in Washington and several Northern California counties surrounding the San Francisco Bay area. The greatest insured losses occurred in Sonoma County, by no means the most populous area in the western United States, but one whose rivers are prone to significant flooding (Ralph et al. 2003).

Spatial plots of total insured losses aggregated over a finer 1/8° grid (not shown) revealed that insured losses were concentrated along the Pacific coast, with large clusters of insured losses corresponding to the urban areas of Seattle, Portland, the San Francisco Bay area,

TABLE 1. Most affected counties, insured losses, and insured losses per coverage.

	County	State	Insured losses (millions USD)	No. of claims	Loss per policy (USD)	Loss per $100,000 coverage (USD)
1	Sonoma	CA	172.0	6650	1324.65	635.66
2	Los Angeles	CA	106.1	8279	114.76	43.23
3	Lewis	WA	99.0	1872	2357.07	1307.87
4	Marin	CA	73.2	3152	320.34	121.40
5	King	WA	69.0	2915	410.57	144.27
6	Sacramento	CA	56.9	3609	33.25	12.43
7	Boulder	CO	54.4	1729	538.27	208.71
8	Snohomish	WA	43.7	1818	675.61	325.06
9	Monterey	CA	43.5	1253	671.83	261.18
10	Napa	CA	43.2	1331	687.31	275.27
11	Washoe	NV	42.4	720	648.17	233.82
12	Maricopa	AZ	33.7	2368	51.50	25.39
13	Santa Clara	CA	33.4	1557	57.58	25.59
14	Clackamas	OR	31.5	730	609.04	230.56
15	San Diego	CA	30.7	1945	126.57	51.62
16	Orange	CA	28.4	3565	20.74	10.10
17	Riverside	CA	27.9	1619	122.97	54.49
18	Cowlitz	WA	26.6	708	241.65	117.38
19	Placer	CA	26.5	598	731.75	257.71
20	Columbia	OR	24.5	395	1869.76	918.86

Los Angeles, and San Diego. Insured losses also clustered around river systems, such as the Willamette River system in Oregon, the Columbia River along the border of Oregon and Washington, the convergence of the San Joaquin and Sacramento Rivers at Sacramento and the San Francisco Bay Delta, and at the windward bases of orographic mountain ranges such as the Cascades in the Pacific Northwest, the Coastal Ranges from Washington to California, the Sierra Nevada in California, the Transverse Range in Southern California, and the Mogollon Rim in Arizona.

Inland insured losses were uniformly low (Fig. 2a), while there were many grid points with high insured losses per coverage in the interior states (Fig. 2b).
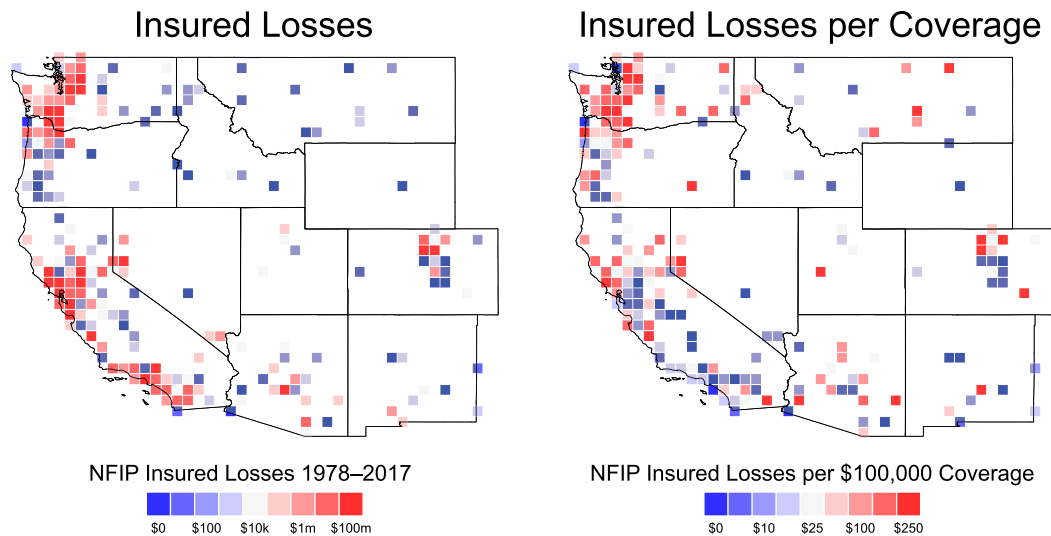

FIG. 2. Spatial distribution of insured losses; payment per coverage. Total insured losses aggregated spatially over a 0.5° grid were concentrated in developed areas in California, Oregon, and Washington. High losses were also observed in Arizona, Colorado, and isolated areas throughout the West. Insured losses per $100,000 coverage were still clustered around developed areas but showed a more even distribution across the West. Insured losses per coverage were lower in Southern California and the Bay Area where population densities are high. Only those grid cells with at least 40 claims over the 40-yr sample period are shown.
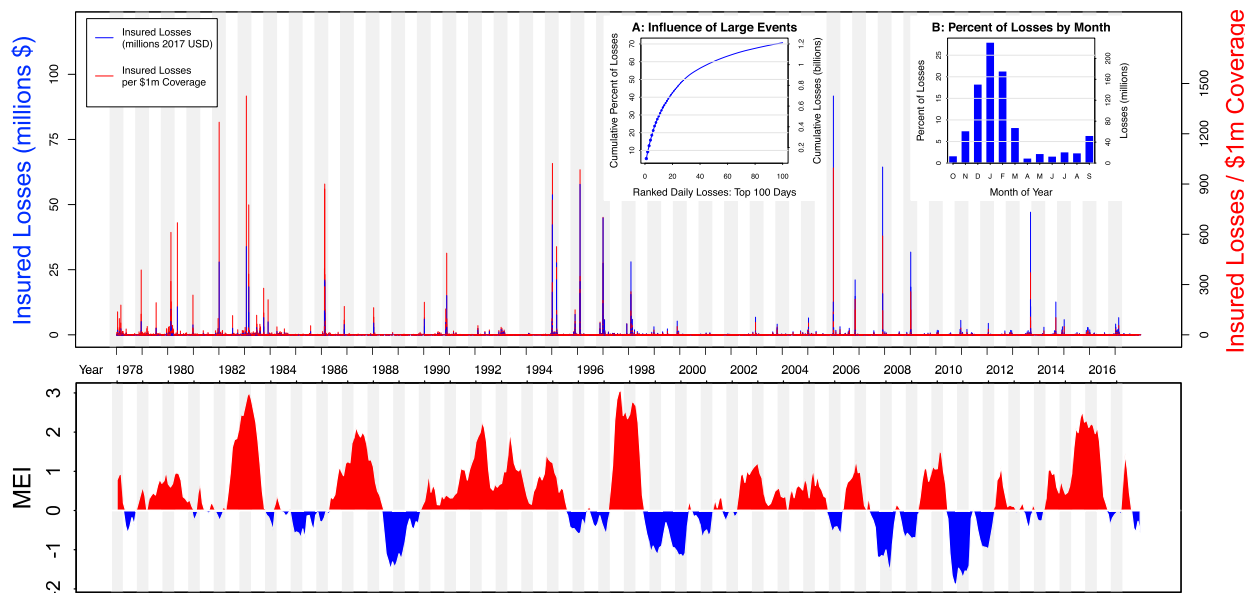
Daily Insured Flood Losses, 11 Western States

FIG. 3. (top) Daily time series of insured losses for 11 western states, 1978–2017. Daily time series of insured losses in blue and insured losses per coverage in red reveal the highly episodic nature of damaging floods in the western United States. Inset A reinforces this finding showing the fraction of losses accounted for by the top 100 loss days. Inset B shows the seasonal pattern of losses across the West. (bottom) MEI over the sample period.

We note that participation rates and number of policyholders were very low in these regions, so we caution against any strong interpretation of these observations.

c. History of insured losses

Inspection of the time series of daily insured losses aggregated over the entire western United States reveals several points of interest (Fig. 3). While there is some weak evidence for a slight increase in insured losses over the sample period, the trend in the time series of insured losses per coverage is in fact negative over our sample period. Perhaps most striking, however, is the highly episodic nature of floods in the western United States: a very small number of extreme events accounted for a great proportion of total insured losses (Fig. 3; see also inset A therein). Insured losses in the western United States displayed a marked seasonal pattern: the coastal areas dominated the aggregate loss data with peak losses occurring between November and March (Fig. 3, inset B).

On average, the inflation-adjusted insured losses from the NFIP amounted to roughly $41.7 million per year ($1.25 billion in total direct damages), although the record was dominated by a handful of large events. The time series exhibits a slight increasing trend over time: the annual growth rate was 1.70% per year from 1978 to 2017 (although, with a standard error of 1.77%, the

trend is not statistically significant). The red bars in Fig. 3 represent insured losses adjusted for the total coverage in force. In this time series of insured losses per coverage the annual growth rate was −4.3%. With a standard error of 1.77%, this rate is significant at the 5% level.

Although inflation-adjusted insured losses associated with flood events in the western United States have remained stationary over the past 40 years, insured losses per coverage have decreased. This may indicate some success of the NFIP program in controlling flood risks in participating communities in the western United States, through repetitive loss buy-back programs and community flood mitigation efforts. Alternatively, it may reflect increased actuarial rates or coverage levels per policy not matched by increases in insured losses. Another possibility is that the residential properties most susceptible to flood damages were damaged in the earlier extreme events of the sample period and either strengthened or not rebuilt.

Weather and hydrologic conditions are characterized by large seasonal to interannual variability, with only moderate long-term trends reported in recent studies. For example, Easterling et al. (2017) report that while annual precipitation averaged across the United States has increased approximately 4% over 1901–2015, parts of the Southwest have declined by 5%–15%.

TABLE 2. Flood events with insured losses in excess of $10 million. S.CA, Southern California; N.CA, Northern California.

	Date	Days	Insured losses ($ in millions)	No. of claims	Loss per $100,000 coverage	Claims per state									MEI
						AZ	S.CA	N.CA	NV	OR	WA	ID	CO	NM	
1	6 Jan 1995	8	119.71	4291	227.8	1	583	3693	5	9	0	0	0	0	1.22
2	30 Dec 2005	4	114.73	2513	124.67	0	20	2187	171	122	13	0	0	0	−0.55
3	3 Feb 1996	15	104.31	2945	177.88	0	3	56	4	1197	1568	84	0	0	−0.57
4	31 Dec 1996	7	98.65	3154	168.24	0	10	2206	411	304	183	30	0	0	−0.33
5	30 Nov 2007	10	84.5	1477	77.42	1	0	8	0	444	1024	0	0	0	−1.15
6	9 Sep 2013	9	76.95	2201	60.63	10	1	1	1	1	1	0	2138	44	−0.13
7	8 Mar 1995	5	58.49	2337	111.29	6	416	1899	12	0	1	1	0	0	0.85
8	5 Jan 2009	7	54.56	1666	44.22	0	0	0	0	14	1646	4	0	0	−0.71
9	17 Feb 1986	6	53.87	1671	230.28	0	14	1575	68	5	3	0	0	0	−0.18
10	1 Feb 1998	5	47.72	2578	43.83	0	447	2126	0	0	4	0	0	0	2.78
11	4Nov 2006	7	39.17	1205	39.45	0	0	0	0	123	1081	1	0	0	1.30
12	25 Jan 1983	5	34.77	1542	146.22	1	472	1043	0	13	11	0	0	1	2.68
13	27 Feb 1983	6	28.85	1742	121.33	9	688	1038	1	4	2	1	0	0	2.93
14	3 Jan 1982	5	28.14	1424	127.69	0	7	1415	0	1	0	1	1	0	−0.26
15	12 Feb 1986	5	23.87	848	102.02	0	58	779	7	2	2	0	0	0	−0.18
16	23 Nov 1990	7	20.63	829	66.62	0	0	0	0	0	825	3	0	0	0.40
17	13 Feb 1980	5	18.84	1298	117.02	248	826	212	0	2	3	0	2	0	0.60
18	6 Feb 1998	8	16.96	1447	15.58	3	399	1041	0	0	2	1	0	0	2.78
19	27 Nov 1995	7	15.77	716	30.01	0	0	2	0	23	684	7	0	0	−0.46
20	7 Sep 2014	3	14.03	288	11.44	190	4	77	16	0	0	0	0	0	0.59
21	9 Jan 2005	7	11.73	522	12.75	7	369	120	21	1	0	0	0	0	0.33
22	18 May 1980	3	11.18	200	69.42	1	0	2	0	2	194	0	1	0	0.97
23	1 Oct 1983	5	10.17	273	42.78	258	4	6	1	0	1	0	0	0	0.06

Increased precipitation intensity over California and other parts of the western United States have been reported by Mass et al. (2011) and Kunkel (2003), but in the Southwest, Prein et al. (2016) find that, since 1980, increases in intensity have been overwhelmed by a decline in the frequency of precipitation-bearing weather types.

As seen in Fig. 3, and displayed in inset A therein, a small number of extreme flood events accounted for a large and disproportionate amount of the insured losses over the past 40 years. The top 28 days of insured losses (constituting 16 separate meteorological events) accounted for over 50% of the insured losses in the western United States over the 40-yr sample period. Events causing over $10 million in insured losses occurred, on average, once every one to two years, although in several cases two such events occurred over the course of a single water-year or even a single month. Assuming that insured losses account for 3.3% of total damages, this translates into total direct damages of approximately $300 million or more per event. Although the western U.S. flood loss history is not as pronounced as, for instance, the record of hurricane damages in the Gulf Coast, it does show a similar highly episodic general form.

The five greatest single-day losses occurred, in order of decreasing insured losses, on 31 December 2005,

3 December 2007, 8 February 1996, 10 January 1995, and 12 September 2013. Table 2 presents a list of the 23 most damaging events over the past 40 years, arranged by date, listing the start dates of the events, the location, the number of claims, total insured losses, and insured losses per $100,000 coverage. Here we define a single event as a set of consecutive days of losses in a given area. All of the significantly damaging events in our record were characterized by a marked peak loss date. In the cases in which two distinct peak loss dates are observed, the successive peaks are classified as separate events (e.g., 12 and 17 February 1986, and 1 and 6 February 1998).

The typical length of a highly damaging flood event in the western United States, as measured from trough to trough in insured losses, was 5 to 10 days. Insured losses per event (in year 2017 USD) were as high as $120 million, which translates into total damages in excess of $1 billion. The estimate on total damages is highly imprecise, but the order of magnitude seems plausible given other estimates in the literature (e.g., Perry 2005). Insured losses per coverage in these highly damaging events varied widely from $12 to $230 per $100,000 worth of coverage.

Regionally, these most damaging events covered a wide geographic area, from Southern California to Washington. We capture the regionality of events in

Month with Most Claims
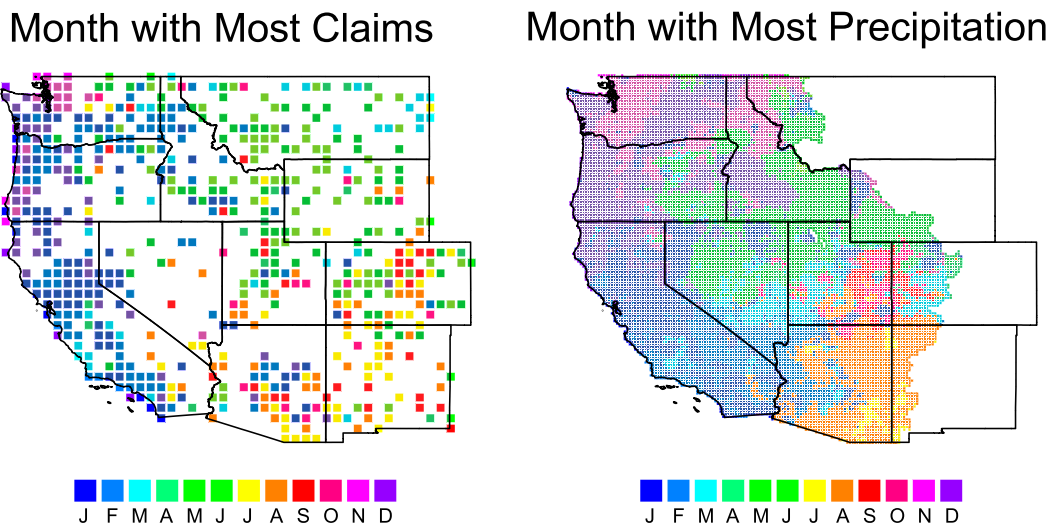
Month with Most Precipitation

FIG. 4. Regional seasonality of flood losses. (left) Total claims were aggregated by month over a 0.5° grid. For each grid cell, the month with the maximum number of claims was noted and is plotted here by color. (right) Total precipitation from 1978 to 2011 was aggregated by month over a 1/8° grid (Livneh et al. 2013; Maurer et al. 2002). For each grid cell, the month with the maximum precipitation was noted and is plotted here by color.

Table 2 by listing the number of claims during the event by region. The top events were concentrated in Northern California, although roughly a third of the top events were associated with significant losses in Washington and Oregon. The link between El Niño and insured losses is explored further below, but there is some evidence of an ENSO influence on losses in these top events. Several of the events concentrated in Southern California were associated with high MEI values, while the top two events concentrated in the Pacific Northwest were associated with low MEI values. Indeed, the strong El Niño damage events (MEI > 2.7) were all concentrated in Southern California. The signal is not perfect, however. Northern California flooding occurred in months with high and low MEI values. The event of 4 November 2006, concentrated in the Pacific Northwest, occurred in a month with elevated MEI (i.e., El Niño conditions).

Insured losses displayed a strong seasonal pattern, as highlighted in Fig. 3 (inset B), with over 84% of total insured losses occurring during the months of October through March, and over 49% in the months of January and February alone. This strong winter flood seasonality was dominated by the large events that occurred along the Pacific coast. The timing of regional peak flood seasons across the western United States was more variable, following a relatively clear general pattern associated with elevation and latitude, as depicted in Fig. 4.

The 40 years of the NFIP record exhibited a progression of winter peak insured losses along the West

Coast, earlier in the winter in the north to later in winter in the south, in accord with the seasonal development and migration of the North Pacific winter storm track (Gershunov et al. 2017). November marked the beginning of the peak flood damage season in the Pacific Northwest, with damaging floods occurring to the east of Puget Sound and at various points along the Pacific coast of Washington and Oregon. Damaging winter flooding (December–February) occurred across the entire western U.S. December peak insured losses occurred in the Olympic Range of western Washington, and along the Pacific coast of Washington and Oregon, and at some locations in Northern California. In January peak insured losses occurred in some locations in all 11 western states. Insured losses caused by January floods were concentrated in central and Northern California, especially surrounding the Bay Delta, but reaching eastward as far as western Nevada. February peak insured losses were concentrated in Southern California, some parts of Northern California, and along the Columbia River valley from northern Idaho through Washington and Oregon. In March, peak insured losses registered in a few locations in Southern California.

Peak losses over the interior West exhibited a more complicated seasonal pattern than those along the West Coast. Peak spring insured losses (March–May) occurred in locations throughout the interior West. Damaging flooding occurred in the spring in northern Washington east of the Cascades, across Montana, Idaho, Wyoming, northern Nevada, Utah, Colorado, and parts of New Mexico. Summer insured losses
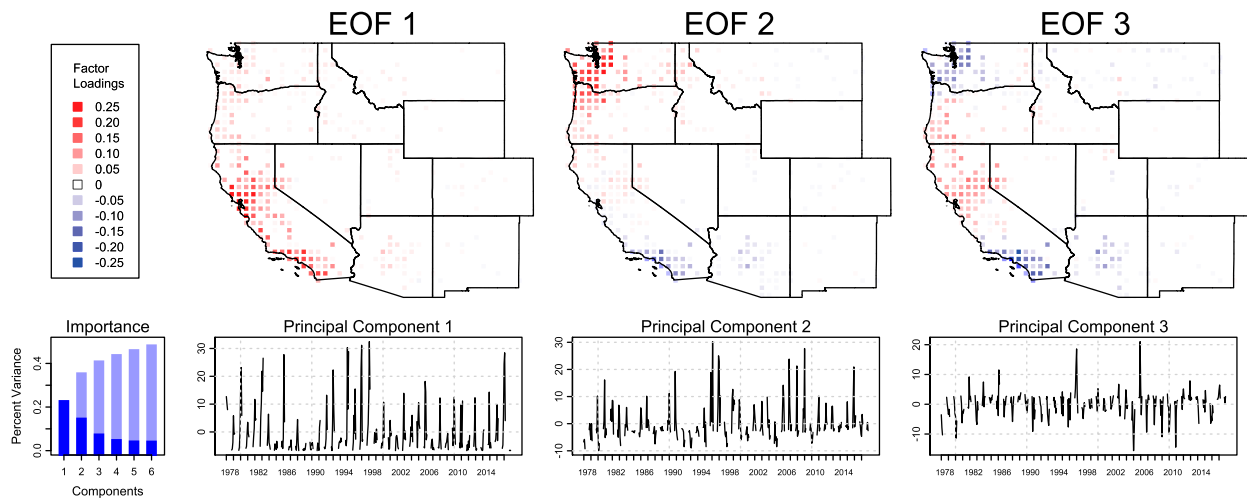
FIG. 5. Principal component analysis (PCA): Cool season log insured losses per coverage over a 0.5° grid. We plot the first three EOFs and PCs of a PCA of monthly insured losses per coverage over the extended cool season (ONDJFM), and the total (dark blue) and cumulative (light blue) percent of the variance explained by the first six components.

(June–August) were relatively rare in the western United States, and appear confined to the Intermountain West, presumably due to smaller-scale convective thunderstorm systems. Damaging floods in July and August occurred in the desert areas of inland Southern California, southern Nevada, and across Arizona, New Mexico, and southern and central Colorado. Fall insured losses (September–November) were concentrated in Arizona, probably a result of the southwest monsoon, remnant tropical storms, and extratropical systems including cutoff lows, with isolated fall insured losses occurring throughout the Intermountain West. December, January, and February peak insured losses occurred, in rather scattered fashion, across the interior West from Arizona and New Mexico northward to Idaho and Montana.

d. Climate linkages

Over a multidecade record, storm events in given regions occur with reasonably well-known frequencies and magnitudes. Superficially their year-to-year occurrences may appear random. But there is a body of research that indicates that large-scale climate anomalies affect the frequencies, intensities, and spatial distribution of the storm systems (e.g., Liu et al. 2018; Fierro 2014; Di Lorenzo et al. 2010; Seager et al. 2005; Thompson and Wallace 2001; Cayan et al. 1999). Here we seek to investigate regional coherence in insured losses and quantify the extent to which ENSO, the most prominent mode of interannual climate variability, is correlated with these losses. We also assess the viability of using ENSO signals in antecedent months to predict insured losses in the western United States The climate linkage

analyses are restricted to insured losses during the extended cool season of ONDJFM, since, as shown in section 4c, it contained 84.4% of the insured losses over the western United States.

To characterize the spatial and temporal patterns of insured losses, we conduct a principal components analysis (PCA) of the 40-yr NFIP record of ONDJFM insured losses per coverage. The PCA demonstrates that insured losses tended to occur over broad regional footprints, as indicated in Fig. 5 by the first three empirical orthogonal functions (EOFs) of ONDJFM monthly insured losses per coverage, aggregated over a 0.5° grid, and their associated monthly PC time series. The first three EOFs accounted for over 40% of the total ONDJFM monthly variance in insured losses. These patterns, respectively, describe flood damage over the coastal communities of Washington, Oregon, and California, over the Pacific Northwest contrasted with central and Southern California, and over coastal Washington and the Southwest contrasted with central and Northern California and coastal southern Oregon. The large spatial footprint of insured losses exhibited in the principal component analysis suggests the influence of climate variability on economically damaging floods.

EOF1, which has same-sign loadings over much of the far western conterminous United States, represents the overall mean pattern in cool season insured losses per coverage, as illustrated in Fig. 2. Factor loadings were highest in Northern California. Factor loadings were of the same sign in Southern California and the Pacific Northwest but of lower magnitude, owing to the higher population densities and coverage levels in those
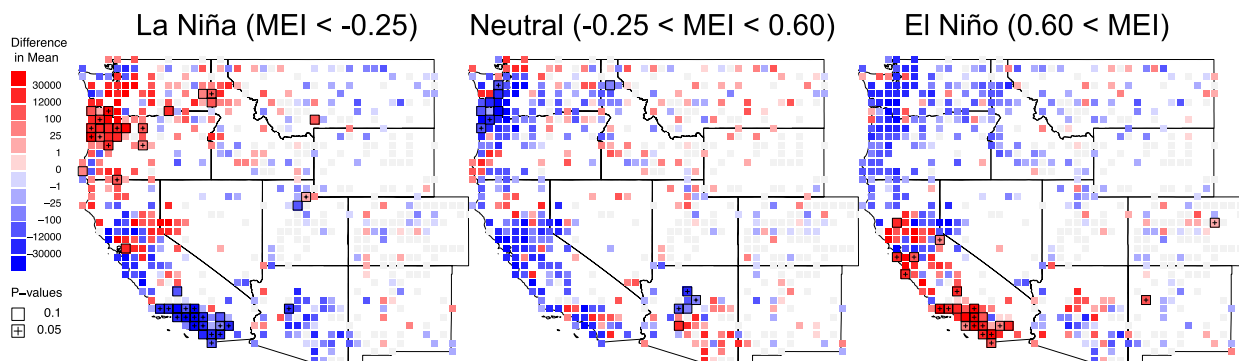
FIG. 6. ENSO composites and mean ONDJFM monthly losses per $100,000 of coverage. We plot composites of mean ONDJFM monthly insured losses per coverage over a 0.5° grid. Enhanced losses are colored red and reduced losses are blue, with color intensity on a log scale. Boxed grid cells are significantly different from the overall ONDJFM mean at $p < 0.1$, using analysis of means (ANOM) analysis. Boxed cells with crosses are significant at $p < 0.05$.

regions. The PC1 time series (associated with EOF1) was elevated in those years with high losses in the areas of greatest variability of losses.

EOF2 is a pronounced north–south dipole, with enhanced factor loadings in the Pacific Northwest extending eastward weakly through the Columbia River basin into northern Idaho and western Montana. The PC2 time series exhibits a strong influence of the 1996 La Niña winter, which was associated with the highest Pacific Northwest losses over the 40-yr period. PC2 also factors negatively during El Niño winters such as 1983 and 1998, resulting in heightened losses in California and diminished losses in the Pacific Northwest in those years.

EOF3 captures variability orthogonal to the first two factors, with positive factor loadings in Northern California. Here the interpretation of the associated time series is complicated by the fact that this component is orthogonal to the first two, although like the previous two PCs it demonstrates the same impacts of extreme events. Correlations with MEI are 0.25, −0.18, and −0.24 for PC1, PC2, and PC3 respectively ($p < 0.01$ in each case), indicating a strong ENSO influence on the primary components of variability in insured losses.

Because ENSO variability was clearly associated with the defined patterns of anomalous precipitation and insured losses across the western United States, this linkage is explored in greater detail. Composites of winter insured losses per coverage, conditional on the contemporaneous MEI (Fig. 6), reveal a strong spatial pattern linking insured losses to the ENSO climate cycle. The El Niño ONDJFM months (MEI > 0.60) exhibited a marked increase in insured losses in coastal Southern California, while insured losses were average or below average in the Pacific Northwest. For the La Niña ONDJFM months (MEI < −0.25) the opposite

pattern emerges, with above-average insured losses in the Pacific Northwest, and below-average insured losses in Southern California, and parts of the Southwest. The cutoff values for MEI were chosen to break the sample of 40 years of ONDJFM months into thirds.

The variable plotted in Fig. 6 is the difference between mean winter monthly insured losses per $100,000 of coverage by ENSO phase, and the overall winter mean. To assess the significance of the differences we use analysis of means (ANOM) to test mean values of the logarithm of insured losses per coverage in each ENSO group to the grand mean over all groups. This is done for each 0.5° grid cell. Significance levels of 0.1 are boxed, and significance levels of 0.05 are marked with plus signs. We note that the statistical significance of the results is not especially strong, particularly considering issues with multiple testing, but the overall spatial coherence of the areas of significance is apparent.

In the La Niña composite we observe increases in losses relative to overall means in coastal northern Oregon, coastal southern Washington, and inland along the Columbia River basin, extending eastward as far as the Idaho Panhandle. There were also scattered areas of increases in losses in southern Oregon and Northern California. Also notable were increased losses on the leeward side of the Sierra Nevada mountain range in California and surrounding Reno along the Truckee River in Nevada. Losses were significantly lower than normal in Southern California and lower in Arizona during the La Niña phase.

In the ENSO-neutral composite we see below-average losses throughout the coastal states. Northwest Oregon and southwest Washington, areas which saw significantly above-average losses in the La Niña phase, saw significantly below-average losses in the ENSO-neutral phase. Losses in Northern California, which displayed

a mixed signal in La Niña months, were consistently and coherently lower than average in the ENSO-neutral phase. ENSO-neutral losses in Southern California and Arizona were mixed. In the interior West, insured losses were weakly above average.

In the El Niño composite we observe significant increases in losses relative to overall mean in coastal Southern California. In the Bay Area east to Sacramento and the Central Valley the signal was mixed. Lower than average losses were observed throughout the Pacific Northwest. Overall, three major patterns emerge. The strongest signal is in Southern California with significantly lower losses in La Niña months and significantly higher losses in El Niño months. A separate pattern emerges in the Pacific Northwest, particularly in northwest Oregon and western Washington, where losses are highest in La Niña months and lowest in ENSO-neutral months, but also below average in El Niño months. Finally, the signal in Northern California is complex with increased losses in some areas during La Niña conditions, generally decreased losses during ENSO-neutral conditions, and increased losses in some area during El Niño conditions.

Given the persistence of different ENSO phases and their influence on insured losses in Southern California and parts of the Pacific Northwest, we next consider how effectively ENSO indices could be used to predict flood insurance claims or insured losses, and how far ahead such predictions could be made.

We calculate the monthly correlations between insured losses by region with MEI over all months of the year over the 40-yr sample period (Fig. 7). Pearson correlations in Washington and Oregon were consistently negative from 0 to 7 months ahead. Correlations of approximately -0.1 were marginally significant ($p < 0.1$) up to 3 months ahead of time. Correlations in Northern California were positive, from 0.05 to 0.1 from 0 to 10 months ahead, but not statistically significant at the 10% level. Correlations in Southern California were positive (0.1 to 0.2) from 0 to 8 months ahead, and strongly significant ($p < 0.01$).

The temporal correlations of MEI with insured losses by region agree with the spatial composites presented above (Fig. 6). The mixed spatial signal in Northern California corresponds to low to moderate and statistically insignificant correlations between leading MEI and losses. The moderate and weakly significant signal in the Pacific Northwest corresponds to the moderate and weakly significant correlations between leading MEI and losses in Washington and Oregon. And the strong signal in Southern California corresponds to strong and significant correlations between leading MEI and losses.
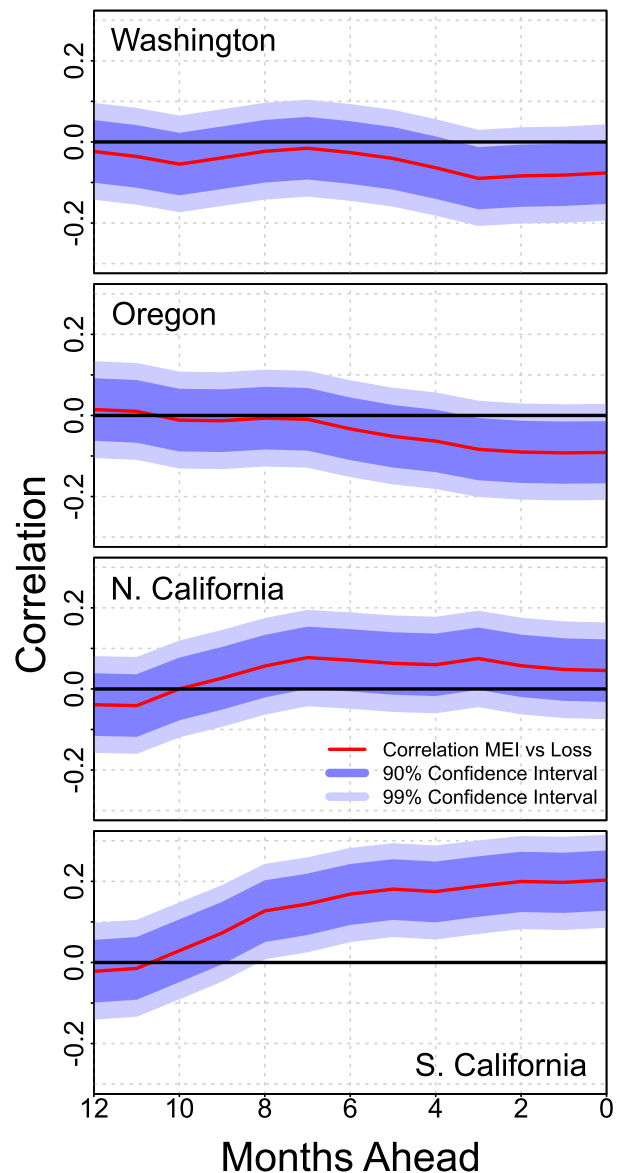

FIG. 7. Correlations of monthly insured losses vs contemporaneous and leading monthly MEI. Strongly significant ($p < 0.01$) positive correlations are seen in Southern California up to 8 months ahead of time. The signal is positive but not significant in Northern California. Negative and weakly significant ($p < 0.1$) correlations are seen in Oregon and Washington up to 3 months ahead.

A possible explanation for the relatively long lead time of positive correlations in Southern California and the shorter lead times of negative correlations in Washington and Oregon is the ENSO spring predictability barrier (Lai et al. 2018). Skillful forecasts of January to March conditions are possible up to 8 months ahead. Combined with the fact that the peak flood damage season in Southern California (January to March) occurs three months after the flood damage season in

Washington and Oregon (October to December), this may partially explain the observed results.

The results above indicate that ENSO forecasts of insured losses up to 6 to 8 months ahead of peak season losses in Southern California may be possible. Such forecasts would be of considerable value to property owners and policy makers, allowing for mitigation activities to be planned and implemented well ahead of winter seasons with highly damaging extreme storm events.

5. Conclusions

Over the 11 states in the conterminous western United States, NFIP losses amounted to about 3.3% of annual losses reported by the NWS. Over the 1983–2003 period, annual losses reported by the NFIP were well correlated with those in the NWS series, indicating that the NFIP insured loss series is a reasonable proxy for total losses in the region. The connection between the two series appeared strongest in those areas where losses were greatest and where population densities were highest.

An examination of the time series of NFIP losses reveals a highly variable pattern of losses from year to year in all locations that experienced any significant flood activity. This underscores the need for the continued federal provision of flood insurance. In spite of recent increases in the provision of private flood insurance (Kousky et al. 2018), it is unlikely that private insurers would be willing or able to underwrite all of the flood risk in the United States. While other studies have found that national flood damages have been increasing dramatically over time, we find only a modest increase in insured losses in the western United States, most of which can be attributed to increased levels of exposure. While the NFIP flood damage measures have not exhibited marked secular trends, they do contain significant temporal and spatial variability. Insured flood losses in the western United States are highly seasonal, with aggregate losses dominated by the seasonality of losses in the coastal states of California, Oregon, and Washington, where insured losses were concentrated over the months of November to March. Further inland, the peak flood season shifts from the winter months to the summer months and total losses decrease markedly.

In spite of the short time sample and the fact that ENSO teleconnections are known to waver, we observe a clear fingerprint of ENSO on the history of insured flood losses in our sample. The patterns associated with ENSO and extreme hydrologic events in the western United States carry over very closely to actual economic impacts. The total variation in losses over time in a given region is high. This said, we find that the ENSO phase

contributes significantly to this variation in the focal areas of Southern California and Arizona, and in the Pacific Northwest, Idaho, and Nevada. In many areas, mean losses in the dominant ENSO phase were several times greater than mean losses in the quiescent phase. Southern California insured losses exhibited the greatest response to ENSO over our sample period, with average losses during El Niño winters over 20 times as great as losses during La Niña winters.

The fact that average annual losses vary substantially between ENSO phases in certain regions raises the possibility that, as property owners become more sophisticated consumers of climatologic forecasts, they may begin to purchase insurance only in those winters where expected losses are high, which could adversely affect the economic sustainability of the NFIP. In a purely market-based insurance program, one might expect to see insurers varying their premium rates on the basis of long-lead climate forecasts. It is unclear whether such a scheme would be feasible or even desirable for the NFIP. A possible alternative to time-varying premium rates would be a further strengthening of mandatory purchase requirements, for example requiring continual coverage in high-risk areas, or only offering contracts of durations longer than one year.

The NFIP data combined with weather, climate, and hydrologic data could be used to address some related economic questions. How and why have NFIP participation rates varied across the West, region by region, and county by county? How do significantly damaging flood events influence participation rates? What other factors influence the local and regional demand for flood insurance? NFIP data have recently been used by Czajkowski et al. (2017) to assess future freshwater flood risk from North Atlantic tropical cyclones. Similar analyses could be conducted to predict the effects of a changing climate on damaging floods in the western United States.

Beyond the ENSO connections that were addressed in this paper, there are important research questions regarding the effects of other forms of weather and climate extremes in causing flood damages in the western United States. A damage function could be developed, linking precipitation, runoff, and antecedent hydrologic conditions with demographic and economic measures of exposure to risk, in order to estimate expected insured flood losses by region. A related direction would be to investigate the importance of driving meteorological phenomena including atmospheric rivers (e.g., Ralph et al. 2019), remnant tropical storms, cutoff low pressure systems, the North American monsoon, mesoscale convective systems, and winter storm surge associated with king tides for coastal flooding.

A significant difficulty in assessing climate risks in terms of extreme flood events is the lack of consistent data on such events. In this study we have demonstrated that NFIP data in combination with climatologic data can yield interesting and powerful results. This research demonstrates the utility of such an interdisciplinary approach and can be extended to quantify the social and economic impacts of a wide variety of meteorological and climatological phenomena across the United States. The continued exploration of the links between climatology, hydrometeorology, and economic impacts is essential in understanding the impacts of anthropogenic climate change as a driver of extreme events over the coming decades.

REFERENCES

Andrews, E. D., R. C. Antweiler, P. J. Neiman, and F. M. Ralph, 2004: Influence of ENSO on flood frequency along the California coast. *J. Climate*, **17**, 337–348, https://doi.org/10.1175/1520-0442(2004)017<0337:IOEOFF>2.0.CO;2.

Cayan, D. R., and D. H. Peterson, 1989: The influence of North Pacific atmospheric circulation on streamflow in the West. *Aspects of Climate Variability in the Pacific and the Western Americas*, *Geophys. Monogr.*, Vol. 55, Amer. Geophys. Union, 375–397, https://doi.org/10.1029/GM055p0375.

——, M. D. Dettinger, H. F. Diaz, and N. Graham, 1998: Decadal variability of precipitation over western North America. *J. Climate*, **11**, 3148–3166, https://doi.org/10.1175/1520-0442(1998)011<3148:DVOPOW>2.0.CO;2.

——, K. T. Redmond, and L. G. Riddle, 1999: ENSO and hydrologic extremes in the western United States. *J. Climate*, **12**, 2881–2893, https://doi.org/10.1175/1520-0442(1999)012<2881:EAHEIT>2.0.CO;2.

Changnon, S., 2003: Measures of economic impacts of weather extremes. *Bull. Amer. Meteor. Soc.*, **84**, 1231–1235, https://doi.org/10.1175/BAMS-84-9-1231.

——, R. A. Pielke Jr., D. Changnon, R. T. Sylves, and R. Pulwarty, 2000: Human factors explain the increased losses from weather and climate extremes. *Bull. Amer. Meteor. Soc.*, **81**, 437–442, https://doi.org/10.1175/1520-0477(2000)081<0437:HFETIL>2.3.CO;2.

Czajkowski, J., G. Villarini, M. Montgomery, E. Michel-Kerjan, and R. Goska, 2017: Assessing current and future freshwater flood risk from North Atlantic tropical cyclones via insurance claims. *Sci. Rep.*, **7**, 41609, https://doi.org/10.1038/srep41609.

Dettinger, M. D., D. R. Cayan, H. F. Diaz, and D. M. Meko, 1998: North–south precipitation patterns in western North America on interannual-to-decadal timescales. *J. Climate*, **11**, 3095–3111, https://doi.org/10.1175/1520-0442(1998)011<3095:NSPPIW>2.0.CO;2.

——, D. S. Battisti, R. D. Garreaud, G. J. McCabe, and C. M. Bitz, 2001: Interhemispheric effects of interannual and decadal ENSO-like climate variations on the Americas. *Interhemispheric Climate Linkages: Present and Past Climates in the Americas and their Societal Effects*, V. Markgraf, Ed., Academic Press, 1–16, https://doi.org/10.1016/B978-012472670-3/50004-5.

Di Lorenzo, E., K. M. Cobb, J. Furtado, N. Schneider, B. Anderson, A. Bracco, M. A. Alexander, and D. Vimont, 2010: Central Pacific El Niño and decadal climate change in the North Pacific. *Nat. Geosci.*, **3**, 762–765, https://doi.org/10.1038/ngeo984.

Dixon, L., N. Clancy, S. A. Seabury, and A. Overton, 2006: The National Flood Insurance Program's market penetration rate: Estimates and policy implications. Technical report, RAND Corporation, accessed 31 December 2018, 116 pp., https://www.rand.org/pubs/technical_reports/TR300.html.

D'Odorico, P., J. C. Yoo, and T. M. Over, 2001: An assessment of ENSO-induced patterns of rainfall erosivity in the southwestern United States. *J. Climate*, **14**, 4230–4242, https://doi.org/10.1175/1520-0442(2001)014<4230:AAOEIP>2.0.CO;2.

Downton, M. W., J. Z. Barnard Miller, and R. A. Pielke Jr., 2005: Reanalysis of U.S. National Weather Service flood loss database. *Nat. Hazards Rev.*, **6**, 13–22, https://doi.org/10.1061/(ASCE)1527-6988(2005)6:1(13).

Easterling, D. R., and Coauthors, 2017: Precipitation change in the United States. *Climate Science Special Report: Fourth National Climate Assessment*, Vol. I, D. J. Wuebbles et al., Eds., U.S. Global Change Research Program, 207–230. https://doi.org/10.7930/J0H993CC.

Emerton, R., H. L. Cloke, E. M. Stephens, E. Zsoter, S. J. Woolnough, and F. Pappenberger, 2017: Complex picture for likelihood of ENSO-driven flood hazard. *Nat. Commun.*, **8**, 14796, https://doi.org/10.1038/ncomms14796.

Fierro, A. O., 2014: Relationships between California rainfall variability and large-scale climate drivers. *Int. J. Climatol.*, **34**, 3626–3640, https://doi.org/10.1002/joc.4112.

Gershunov, A., 1998: ENSO influence on intraseasonal extreme rainfall and temperature frequencies in the contiguous United States: Implications for long-range predictability. *J. Climate*, **11**, 3192–3203, https://doi.org/10.1175/1520-0442(1998)011<3192:EIOIER>2.0.CO;2.

——, and T. P. Barnett, 1998: ENSO influence on intraseasonal extreme rainfall and temperature frequencies in the contiguous United States: Observations and model results. *J. Climate*, **11**, 1575–1586, https://doi.org/10.1175/1520-0442(1998)011<1575:EIOIER>2.0.CO;2.

——, T. Shulgina, F. M. Ralph, D. A. Lavers, and J. J. Rutz, 2017: Assessing the climate-scale variability of atmospheric rivers affecting western North America. *Geophys. Res. Lett.*, **44**, 7900–7908, https://doi.org/10.1002/2017GL074175.

Glantz, M. H., 2001: *Currents of Change: Impacts of El Niño and La Niña on Climate and Society*. 2nd ed. Cambridge University Press, 252 pp.

Groisman, P. Ya., R. W. Knight, D. R. Easterling, T. R. Karl, G. C. Hegerl, and V. N. Razuvaev, 2005: Trends in intense precipitation in the climate record. *J. Climate*, **18**, 1326–1350, https://doi.org/10.1175/JCLI3339.1.

Higgins, R. W., J.-K. E. Schemm, W. Shi, and A. Leetmaa, 2000: Extreme precipitation events in the western United States related to tropical forcing. *J. Climate*, **13**, 793–820, https://doi.org/10.1175/1520-0442(2000)013<0793:EPEITW>2.0.CO;2.

Horn, D. P., and J. T. Brown, 2018: Introduction to the National Flood Insurance Program (NFIP). Congressional Research Service Rep. R44593, 27 pp., https://fas.org/sgp/crs/homesec/R44593.pdf.

Karl, T. R., and R. W. Knight, 1998: Secular trends of precipitation amount, frequency, and intensity in the United States. *Bull. Amer. Meteor. Soc.*, **79**, 231–241, https://doi.org/10.1175/1520-0477(1998)079<0231:STOPAF>2.0.CO;2.

Klotzbach, P. J., S. G. Bowen, R. Pielke, and M. Bell, 2018: Continental U.S. hurricane landfall frequency and associated damage: Observations and future risks. *Bull. Amer. Meteor. Soc.*, **99**, 1359–1376, https://doi.org/10.1175/BAMS-D-17-0184.1.

Kousky, C., H. Kunreuther, B. Lingle, and L. Shabman, 2018: The emerging private residential flood insurance market in the United States. Wharton Risk Management and Decision Processes Center, 51 pp.

Kunkel, K. E., 2003: North American trends in extreme precipitation. *Nat. Hazards*, **29**, 291–305, https://doi.org/10.1023/A:1023694115864.

Kunreuther, H. O., 1998: Introduction. *Paying the Price: The Status and Role of Insurance against Natural Disasters in the United States*, H. O. Kunreuther and R. J. Roth Sr., Eds., Joseph Henry Press, 1–16, https://doi.org/10.17226/5784.

Lai, A. W.-C., M. Herzog, and H. Graf, 2018: ENSO forecasts near the spring predictability barrier and possible reasons for the recently reduced predictability. *J. Climate*, **31**, 815–838, https://doi.org/10.1175/JCLI-D-17-0180.1.

Liu, Y. C., P. Di, S. H. Chen, and J. DaMassa, 2018: Relationships of rainy season precipitation and temperature to climate indices in California: Long-term variability and extreme events. *J. Climate*, **31**, 1921–1942, https://doi.org/10.1175/JCLI-D-17-0376.1.

Livezey, R. E., M. Masutani, A. Leetmaa, H. Rui, M. Ji, and A. Kumar, 1997: Teleconnective response of the Pacific–North American region atmosphere to large central equatorial Pacific SST anomalies. *J. Climate*, **10**, 1787–1820, https://doi.org/10.1175/1520-0442(1997)010<1787:TROTPN>2.0.CO;2.

Livneh, B., E. A. Rosenberg, C. Lin, B. Nijssen, V. Mishra, K. M. Andreadis, E. P. Maurer, and D. P. Lettenmaier, 2013: A long-term hydrologically based dataset of land surface fluxes and states for the conterminous United States: Update and extensions. *J. Climate*, **26**, 9384–9392, https://doi.org/10.1175/JCLI-D-12-00508.1.

Mass, C., A. Skalenakis, and M. Warner, 2011: Extreme precipitation over the West Coast of North America: Is there a trend? *J. Hydrometeor.*, **12**, 310–318, https://doi.org/10.1175/2010JHM1341.1.

Maurer, E. P., A. W. Wood, J. C. Adam, D. P. Lettenmaier, and B. Nijssen, 2002: A long-term hydrologically based dataset of land surface fluxes and states for the conterminous United States. *J. Climate*, **15**, 3237–3251, https://doi.org/10.1175/1520-0442(2002)015<3237:ALTHBD>2.0.CO;2.

McCabe-Glynn, S., K. R. Johnson, C. Strong, Y. Zou, J. Y. Yu, S. Sellars, and J. M. Welker, 2016: Isotopic signature of extreme precipitation events in the western U.S. and associated phases of Arctic and tropical climate modes. *J. Geophys. Res. Atmos.*, **121**, 8913–8924, https://doi.org/10.1002/2016JD025524.

NOAA/National Weather Service, 2018: Hydrologic Information Center 2018: Flood loss data, accessed 31 December 2018, http://www.nws.noaa.gov/hic/.

NOAA/NCEI, 2018: U.S. billion-dollar weather and climate disasters. Accessed 31 December 2018, https://www.ncdc.noaa.gov/billions/.

Pasterick, E. T., 1998: The National Flood Insurance Program. *Paying the Price: The Status and Role of Insurance against Natural Disasters in the United States*, H. O. Kunreuther and R. J. Roth, Eds., Joseph Henry Press, 125–154, https://doi.org/10.17226/5784.

Perry, C. A., 2005: Summary of significant floods in the United States and Puerto Rico, 1994 through 1998 water years. Scientific Investigations Rep. 2005–5194, U.S. Geological Survey, 35 pp.

Philander, S. G., 1990: *El Niño, La Niña, and the Southern Oscillation*. Academic Press, 293 pp.

Pielke, R. A., Jr., and M. W. Downton, 2000: Precipitation and damaging floods: Trends in the United States, 1932–97. *J. Climate*, **13**, 3625–3637, https://doi.org/10.1175/1520-0442(2000)013<3625:PADFTI>2.0.CO;2.

——, ——, and J. Z. Barnard Miller, 2002: Flood damage in the United States, 1926–2000: A reanalysis of National Weather Service estimates. Tech. Rep., Environmental and Societal Impacts Group, NCAR, 86 pp., https://sciencepolicy.colorado.edu/flooddamagedata/flooddamagedata.pdf.

Prein, A. F., G. J. Holland, R. M. Rasmussen, M. P. Clark, and M. R. Tye, 2016: Running dry: The US Southwest's drift into a drier climate state. *Geophys. Res. Lett.*, **43**, 1272–1279, https://doi.org/10.1002/2015GL066727.

Ralph, F. M., P. J. Neiman, D. E. Kingsmill, P. O. Persson, A. B. White, E. T. Strem, E. D. Andrews, and R. C. Antweiler, 2003: The impact of a prominent rain shadow on flooding in California's Santa Cruz mountains: A CALJET case study and sensitivity to the ENSO cycle. *J. Hydrometeor.*, **4**, 1243–1264, https://doi.org/10.1175/1525-7541(2003)004<1243:TIOAPR>2.0.CO;2.

——, J. J. Rutz, J. M. Cordeira, M. D. Dettinger, M. Anderson, D. Reynolds, L. J. Schick, and C. Smallcomb, 2019: A scale to characterize the strength and impacts of atmospheric rivers. *Bull. Amer. Meteor. Soc.*, **100**, 269–289, https://doi.org/10.1175/BAMS-D-18-0023.1 .

Redmond, K. T., and R. W. Koch, 1991: Surface climate and streamflow variability in the western United States and their relationship to large-scale circulation indices. *Water Resour. Res.*, **27**, 2381–2399, https://doi.org/10.1029/91WR00690.

Risser, M. D., and M. F. Wehner, 2017: Attributable human-induced changes in the likelihood and magnitude of the observed extreme precipitation during Hurricane Harvey. *Geophys. Res. Lett.*, **44**, 12 457–12 464, https://doi.org/10.1002/2017GL075888.

Ropelewski, C. F., and M. S. Halpert, 1986: North American precipitation and temperature patterns associated with the El Niño/Southern Oscillation (ENSO). *Mon. Wea. Rev.*, **114**, 2352–2362, https://doi.org/10.1175/1520-0493(1986)114<2352:NAPATP>2.0.CO;2.

Santer, B. D., and Coauthors, 2007: Identification of human-induced changes in atmospheric moisture content. *Proc. Natl. Acad. Sci. USA*, **104**, 15 248–15 253, https://doi.org/10.1073/pnas.0702872104.

Seager, R., N. Harnik, W. Robinson, Y. Kushnir, M. Ting, H. Huang, and J. Velez, 2005: Mechanisms of ENSO-forcing

of hemispherically symmetric precipitation variability. *Quart. J. Roy. Meteor. Soc.*, **131**, 1501–1527, https://doi.org/10.1256/qj.04.96.

Sylves, R. T., 1998: Disasters and coastal states: A policy analysis of presidential declarations of disaster 1953–97. Tech. Rep., University of Delaware Sea Grant College Program, 155 pp.

——, and W. L. Waugh Jr., Eds., 1996: *Disaster Management in the U.S. and Canada: The Politics, Policymaking, Administration, and Analysis of Emergency Management*. Charles C. Thomas, 422 pp.

Thompson, D. W. J., and J. M. Wallace, 2001: Regional climate impacts of the Northern Hemisphere annular mode. *Science*, **293**, 85–89, https://doi.org/10.1126/science.1058958.

U.S. Army Corps of Engineers, 2009: Flood risk management: Value to the nation. U.S. Army Engineer Institute for Water Resources Tech. Rep., 5 pp., https://www.mvk.usace.army.mil/Portals/58/docs/PP/ValueToTheNation/VTNFloodRiskMgmt.pdf.

U.S. Bureau of Economic Analysis, 2018: Gross Domestic Product: Table 1.1.3. Real Gross Domestic Product, Quantity Indexes, as of 26 January 2018, https://apps.bea.gov/itable/index.cfm.

Villarini, G., and L. Slater, 2017: Climatology of flooding in the United States. *Oxford Research Encyclopedia of Natural Hazard Science*, S. L. Cutter, Ed., Oxford University Press, https://doi.org/10.1093/acrefore/9780199389407.013.123.

Wang, S. S., L. Zhao, J. H. Yoon, P. Klotzbach, and R. R. Gillies, 2018: Quantitative attribution of climate effects on Hurricane Harvey's extreme rainfall in Texas. *Environ. Res. Lett.*, **13**, 054014, https://doi.org/10.1088/1748-9326/aabb85.

Ward, P. J., S. Eisner, M. Flörke, M. D. Dettinger, and M. Kummu, 2014a: Annual flood sensitivities to El Niño–Southern Oscillation at the global scale. *Hydrol. Earth Syst. Sci.*, **18**, 47–66, https://doi.org/10.5194/hess-18-47-2014.

——, B. Jongman, M. Kummu, M. D. Dettinger, F. C. Sperna Weiland, and H. C. Winsemius, 2014b: Strong influence of El Niño Southern Oscillation on flood risk around the world. *Proc. Natl. Acad. Sci. USA*, **111**, 15 659–15 664, https://doi.org/10.1073/pnas.1409822111.

——, M. Kummu, and U. Lall, 2016: Flood frequencies and durations and their response to El Niño Southern Oscillation: Global analysis. *J. Hydrol.*, **539**, 358–378, https://doi.org/10.1016/j.jhydrol.2016.05.045.

Westra, S., L. V. Alexander, and F. W. Zwiers, 2013: Global increasing trends in annual maximum daily precipitation. *J. Climate*, **26**, 3904–3918, https://doi.org/10.1175/JCLI-D-12-00502.1.

Wolter, K., and M. S. Timlin, 1998: Measuring the strength of ENSO events: How does 1997/98 rank? *Weather*, **53**, 315–324, https://doi.org/10.1002/j.1477-8696.1998.tb06408.x.